Mixed State of a Dirty Two-Band Superconductor: Application to MgB_2

A. E. Koshelev
Materials Science Division, Argonne National Laboratory, Argonne, Illinois 60439, USA

A. A. Golubov
Department of Applied Physics, University of Twente, 7500 AE Enschede, The Netherlands

(Received 25 October 2002; published 29 April 2003)

We investigate the vortex state in a two-band superconductor with strong intraband and weak interband electronic scattering rates. Coupled Usadel equations are solved numerically, and the distributions of the pair potentials and local densities of states are calculated for two bands at different values of magnetic fields. The existence of two distinct length scales corresponding to different bands is demonstrated. The results provide qualitative interpretation of recent scanning tunneling microscopy experiments on vortex structure imaging in MgB_2.

DOI: 10.1103/PhysRevLett.90.177002 PACS numbers: 74.25.Ha, 74.20.De, 74.25.Op

A very peculiar feature of the recently discovered superconductor MgB_2 [1] is the multigap nature of the superconducting state. The possibility of such a state was first predicted in [2,3] for a multiband superconductor with large disparity of the electron-phonon interaction for the different Fermi-surface sheets. Various aspects of multiband superconductivity, in particular, the role of impurity scattering, were discussed theoretically in [4–7]. For MgB_2, the two-band model was first suggested in [8,9]. First-principles calculations show that superconductivity in this compound resides in two groups of bands: the group of two strongly superconducting σ bands and the group of two weakly superconducting π bands. Quantitative predictions for T_c, energy gaps, specific heat [10,11], and tunneling [12] were made recently.

The signature of two energy gaps was observed in Nb doped $SrTiO_3$ [13]. But to date, only in MgB_2 the existence of two distinct gaps has been most clearly demonstrated. A large number of experimental data, in particular, tunneling [14–16], point contact [17–19], and heat capacity measurements [20], directly support the concept of a double gap MgB_2. It was argued in Ref. [21] that the unexpectedly weak correlation between T_c and the resistivity can be reconciled with the two-band model, if one assumes that the interband impurity scattering remains weak even in samples with strong intraband impurity scattering in the π band. In most presently available MgB_2 samples both bands are probably in the dirty limit. Even in the best available crystals the de Haas–van Alphen data [22] suggest that the σ band is moderately clean and the π band is moderately dirty.

Two-band superconductivity in MgB_2 offers new interesting physics. For example, it was demonstrated that the anisotropies of the upper critical fields and the London penetration depths are different and have opposite temperature dependencies [23]. Recently, the c-axis Abrikosov vortex structure in MgB_2 was studied by scanning tunneling microscopy (STM) [24]. Several important observations have been made: large vortex core size compared to estimates based on H_{c2}, the absence of zero-bias singularity in the core and the rapid suppression of the apparent tunneling gap by magnetic fields much smaller than H_{c2}. It is important to note that c-axis tunneling in MgB_2 probes mainly the π band [15].

In this Letter, we provide a quantitative model for the vortex structure in a dirty two-band superconductor. We demonstrate the existence of two different spatial and magnetic field scales, consistent with the data in [24]. The same conclusions have been reached in Ref. [25] where the vortex structure in a clean two-band superconductor has been studied on the basis of the Bogoliubov–de Gennes equations.

We consider a two-band superconductor with weak interband impurity scattering and rather strong intraband scattering rates exceeding the corresponding energy gaps (dirty limit). In this case the quasiclassical Usadel equations [26] are applicable within each band. The vortex structure in a single-band dirty superconductor was studied extensively in the framework of the Usadel equations [27,28]. To describe the mixed state in the considered case, one can generalize this approach and write down the system of coupled Usadel equations

$$\omega F_\alpha - \frac{\mathcal{D}_\alpha}{2}\left[G_\alpha\left(\boldsymbol{\nabla} - \frac{2\pi i}{\Phi_0}\mathbf{A}\right)^2 F_\alpha - F_\alpha \boldsymbol{\nabla}^2 G_\alpha \right] = \Delta_\alpha G_\alpha, \tag{1}$$

$$\Delta_\alpha = 2\pi T \sum_{\beta,n} \Lambda_{\alpha\beta} F_\beta, \tag{2}$$

where $\alpha = 1, 2$ is the band index, $\hat{\Lambda}$ is the matrix of effective coupling constants (to be defined below), $\mathcal{D}_\alpha$ are diffusion constants, which determine the coherence lengths $\xi_\alpha = \sqrt{\mathcal{D}_\alpha/2\pi T_c}$, G_α and F_α are normal and anomalous Green's functions connected by normalization condition $G_\alpha^2 + F_\alpha^* F_\alpha = 1$, Δ_α is the pair potential, and $\omega = (2n+1)\pi T$ are Matsubara frequencies. Bearing in mind the application to MgB_2, in our notations index 1 corresponds to σ bands and index 2 to π bands.

In the considered case of weak interband scattering the Green's functions in different bands are coupled only indirectly, via the self-consistency Eq. (2). We will show that this leads to the existence of two different length scales in different bands and, as a consequence, two magnetic field scales appear which are directly accessible experimentally. Such a situation has never existed in the field of vortex physics. This is in contrast to the usual proximity effect in real space (e.g., N/S multilayers), where different energy and length scales reside in spatially separated N, S layers.

We study the case when magnetic field is oriented along the c axis. Further, we neglect in-plane anisotropy and adopt a circular cell approximation for the vortex unit cell [27] (see inset in Fig. 1). We also assume a large Ginzburg-Landau parameter $\kappa \gg 1$ (in MgB_2, $\kappa \gtrsim 10$) and consider magnetic fields much larger than the lower critical field, so that we can neglect variations of the magnetic field. We will use reduced variables: energy and length will be measured in the units of πT_c and $\xi_1 = \sqrt{\mathcal{D}_1/2\pi T_c}$, respectively. The distribution of superfluid momentum within the unit cell is then given by

$$p = 1/r - r/r_c^2, \qquad r_c^2 = H_1/H, \qquad H_\alpha \equiv 2T_c\Phi_0/\mathcal{D}_\alpha, \tag{3}$$

where r is the distance from the center of a vortex core.

Using θ parametrization ($F_\alpha = \sin\theta_\alpha$, $G_\alpha = \cos\theta_\alpha$), the Usadel equations and the self-consistency conditions can be rewritten in the form

$$\partial_r^2\theta_\alpha + \frac{1}{r}\partial_r\theta_\alpha - p^2\cos\theta_\alpha\sin\theta_\alpha + k_\alpha^2(\Delta_\alpha\cos\theta_\alpha - \omega\sin\theta_\alpha) = 0, \tag{4}$$

$$W_1\Delta_1 - W_{12}\Delta_2 = 2t\sum_{\omega>0}\left(\sin\theta_1 - \frac{\Delta_1}{\omega}\right) + \Delta_1\ln\frac{1}{t}, \tag{5a}$$

$$-W_{21}\Delta_1 + W_2\Delta_2 = 2t\sum_{\omega>0}\left(\sin\theta_2 - \frac{\Delta_2}{\omega}\right) + \Delta_2\ln\frac{1}{t} \tag{5b}$$

with $k_1^2 = 1$, $k_2^2 = \mathcal{D}_1/\mathcal{D}_2$, $\omega = t(2n+1)$, $t = T/T_c$.

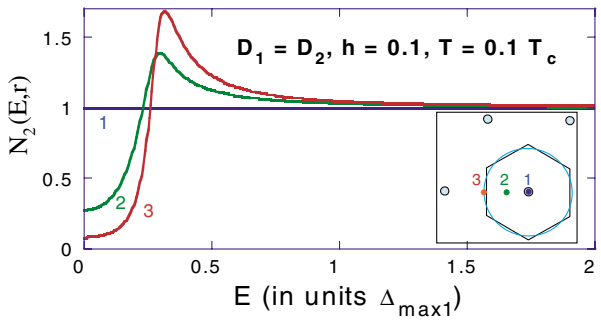

FIG. 1 (color online). Local density of state for π band at different points of vortex lattice unit cell at $h = 0.1$ for $\mathcal{D}_1 = \mathcal{D}_2 = 1$. Inset illustrates the circular cell approximation and shows points at which the spectra are presented.

The matrix $W_{\alpha\beta}$ is related to the coupling constants $\Lambda_{\alpha\beta}$ as

$$W_1 = \frac{-A + \sqrt{A^2 + \Lambda_{12}\Lambda_{21}}}{\mathrm{Det}}, \qquad W_2 = \frac{A + \sqrt{A^2 + \Lambda_{12}\Lambda_{21}}}{\mathrm{Det}}, \qquad W_{12} = \Lambda_{12}/\mathrm{Det},\ W_{21} = \Lambda_{21}/\mathrm{Det}, \tag{6}$$

where $A = (\Lambda_{11} - \Lambda_{22})/2$, $\mathrm{Det} = \Lambda_{11}\Lambda_{22} - \Lambda_{12}\Lambda_{21}$ [29]. Note that only three constants are independent since $W_1W_2 = W_{12}W_{21}$. Partial local densities of states (DOS) $N_\alpha(\varepsilon, r)$, which are accessible in tunneling experiments, can be obtained from $\Theta_\alpha(\omega, r)$ using analytic continuation

$$N_\alpha(\varepsilon, r) = \mathrm{Re}[\cos\Theta_\alpha(i\omega \to \varepsilon + i\delta, r)]. \tag{7}$$

The above set of Eqs. (3)–(7) fully defines the vortex core structure in a diffusive two-band superconductor. In general, a numerical solution is required to determine the behavior of the pair potentials and DOS in both bands. The problem simplifies near the upper critical field when Eqs. (4) can be linearized

$$\partial_r^2\theta_\alpha + \frac{1}{r}\partial_r\theta_\alpha - (1/r - r/r_c^2)^2\theta_\alpha - k_\alpha^2\omega\theta_\alpha = -k_\alpha^2\Delta_\alpha.$$

These equations have exact solution [27]

$$\Delta_\alpha = \Delta_{0\alpha} r\exp(-r^2/2r_c^2), \qquad \theta_\alpha = \theta_{0\alpha} r\exp(-r^2/2r_c^2),$$

giving the relation $\theta_{0\alpha} = \Delta_{0\alpha}/(2/k_\alpha^2 r_c^2 + \omega)$. Substituting this result into the self-consistency equations, we derive the equation for H_{c2},

$$\ln\frac{1}{t} - g\left(\frac{H_{c2}}{tH_1}\right) = -\frac{W_1[\ln\frac{1}{t} - g(\frac{H_{c2}}{tH_2})]}{W_2 - [\ln\frac{1}{t} - g(\frac{H_{c2}}{tH_2})]}, \tag{8}$$

and relation between Δ_{01} and Δ_{02} near H_{c2},

$$\Delta_{02} = \frac{W_{21}\Delta_{01}}{W_2 + \ln\frac{1}{t} - g(\frac{H}{tH_2})}, \tag{9}$$

where $g(x) \equiv \psi(1/2 + x) - \psi(1/2)$ and $\psi(x)$ is a digamma function. In the single-band case the upper critical field H_{c2}^s is given by the standard Maki–de Gennes equation

$$\ln(1/t) = g[H_{c2}^s/(tH_1)]. \tag{10}$$

The electron-phonon interaction in MgB_2 was calculated from first principles in [8,10,11]. In Ref. [11] the matrices of the electron-phonon coupling constants λ_{ij} and the renormalized Coulomb pseudopotentials μ_{ij}^* were derived for the effective two-band model. In this Letter we use these results and define the effective constants $\Lambda_{ij} = \lambda_{ij} - \mu_{ij}^*$ in the weak coupling model, neglecting the strong-coupling corrections, which is a reasonable approximation for our purpose. The corresponding numerical values are [11] $\Lambda_{11} \approx 0.81$, $\Lambda_{22} \approx 0.278$,

$\Lambda_{12} \approx 0.115$, $\Lambda_{21} \approx 0.091$, from which we obtain values of $W_{\alpha\beta}$ used in numerical calculations, $W_1 \approx 0.088$, $W_2 \approx 2.56$, $W_{12} \approx 0.535$, $W_{21} \approx 0.424$. With fixed coupling constants the overall behavior is determined by the ratio of the diffusion constants $\mathcal{D}_1/\mathcal{D}_2$. In this Letter we present calculations for the ratio $\mathcal{D}_1/\mathcal{D}_2 = 0.2$, which gives the best agreement with the experiment of Ref. [24], and for the case of identical transport characteristics in two bands $\mathcal{D}_1/\mathcal{D}_2 = 1$.

The magnetic field is measured with respect to the single-band upper critical field of the σ band, $h \equiv H/H^s_{c2}(t)$, where H^s_{c2} is given by Eq. (10). For the case $W_1 \ll W_2$ realized in MgB_2, the upper critical field is mainly determined by the strong band. A small correction due to the weak band can be found from Eq. (8) using an expansion with respect to the small parameter $S_{12} \equiv W_1/W_2$. In particular, we found very simple expressions for the slope of H_{c2} at T_c and $H_{c2}(0)$:

$$\frac{dH_{c2}}{dT} \approx \frac{dH^s_{c2}}{dT}\left(1 + S_{12}\frac{H_2 - H_1}{H_2}\right),$$

$$H_{c2}(0) \approx H^s_{c2}(0)[1 + S_{12}\ln(H_2/H_1)].$$

With the above parameters, we numerically solved Eqs. (4) and (5a) for different magnetic fields. Figure 1 shows an example of local DOS for the π band at different points of the vortex unit cell. One can see that in the center of the core there is no zero-energy peak in the DOS in the core usually observed in clean superconductors [30]. This property is a consequence of the dirty limit in the π band. As one can expect, the most pronounced dependence on energy is observed at the boundary of the vortex unit cell (curve 3 in Fig. 1). One can see that the DOS is peaked at an energy about 3 times smaller than $\Delta_{\max 1}$. This peak corresponds to the small energy gap in the second band.

We study the structure of an isolated vortex by solving the Usadel equations at very small field ($h = 0.002$). Figures 2(a) and 2(b) show the spatial dependence of the pair potentials, $\Delta_1(r)$ and $\Delta_2(r)$, and their ratio for $t = 0.1$ for two cases: $\mathcal{D}_1 = 0.2\mathcal{D}_2$ and $\mathcal{D}_1 = \mathcal{D}_2$. Figures 2(c) and 2(d) shows the DOS at zero energy, $N_1(0, r)$, and $N_2(0, r)$. One can see that in the case of $\mathcal{D}_1 = 0.2\mathcal{D}_2$ the pair potential and the DOS in the π band demonstrate qualitatively different behavior. The pair potentials approach their bulk values $\Delta_{\alpha,0}$ at the length scale set by the strong band. Δ_1 reaches half of $\Delta_{1,0}$ at $r = 2.15\xi_1$ and Δ_2 reaches half of $\Delta_{2,0}$ at a somewhat larger length scale, $r = 3.44\xi_1$. π-band DOS, $N_2(0, r)$, has significantly longer range: it drops to 0.5 at $r = 6.35\xi_1$. Therefore the relation between $N_2(\epsilon, \mathbf{r})$ and $\Delta_2(\mathbf{r})$ is essentially nonlocal. Though the above numbers correspond to the specific choice of parameters for the coupling matrix Λ_{ij}, the large core size in the weakly superconducting band is the general property of a two-band superconductor.

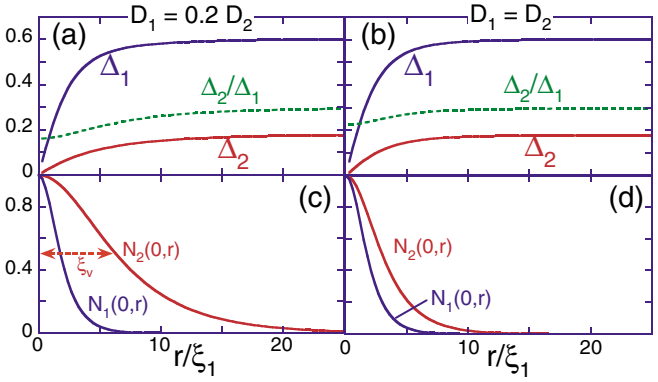

FIG. 2 (color online). Spatial dependencies of pair potentials [(a) and (b)] and partial DOS at $E = 0$ [(c) and (d)] for isolated vortex for two ratios D_1/D_2: $D_1 = 0.2D_2$ and $D_1 = D_2$.

The two typical sizes of the isolated vortex determine the two typical field scales. Figure 3 shows the field dependence of the maximum values of the pair potentials at the boundary of vortex unit cell [3(a) and 3(b)] and DOS at $\epsilon = 0$ averaged over the unit cell [3(c) and 3(d)]. One can see that for the case of $\mathcal{D}_1 = 0.2\mathcal{D}_2$ the average DOS in the π band reaches its normal value at fields considerably smaller than the upper critical field.

Recently, the c-axis vortex structure in MgB_2 single crystals was measured by STM [24]. Most strikingly, it was observed that the spatial extension of the vortex core was a few times larger than the length $\sim$10 nm estimated from H_{c2}. Our model naturally explains this observation. One can see from Fig. 4 that the apparent vortex size can indeed exceed the size estimated from H_{c2}. The magnitude of the enhancement depends on the ratio of the diffusion constants in the two bands. As follows from numerical calculations, the apparent vortex size ξ_v is approximately given by the expression $\xi_v = 2.7\xi_2 + 0.3\xi_1$. The low energy peak (around 2.2 meV) in the region between the vortices and its rapid suppression by magnetic field is also explained by our model.

The measured value of $\xi_v/\xi_{c2} = 3$ corresponds in our model to the ratio $\xi_2/\xi_1 = 2$. We cannot make a

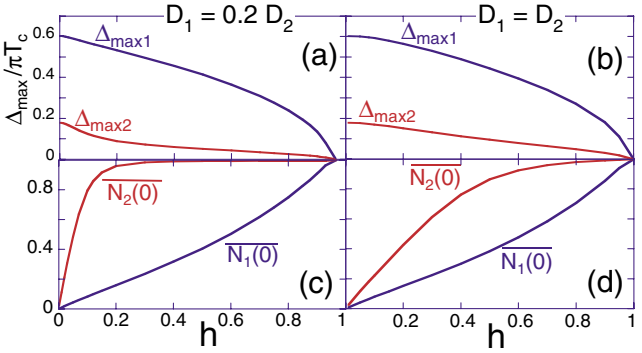

FIG. 3 (color online). Field dependencies of maximum pair potentials [(a) and (b)] and averaged DOS at $\epsilon = 0$ [(c) and (d)] for two ratios D_1/D_2: $D_1 = 0.2D_2$ and $D_1 = D_2$.

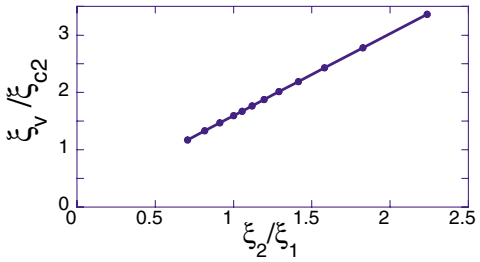

FIG. 4 (color online). Ratio of the apparent vortex size ξ_v as defined in Fig. 2(c) to the coherence length ξ_{c2} extracted from the upper critical field, $\xi_{c2} \equiv \sqrt{\Phi_0/(2\pi H_{c2})}$ plotted vs ratio of the length scales in two bands, $\xi_2/\xi_1 \equiv \sqrt{\mathcal{D}_2/\mathcal{D}_1}$. According to Ref. [24] for MgB_2 single crystal the ratio ξ_v/ξ_{c2} is around 3.

quantitative comparison between the measured and calculated values of ξ_v, since scattering parameters in different bands for MgB_2 single crystals of Ref. [24] are not known. Moreover, the available data on resistivity and the de Haas–van Alphen effect [22] suggest that the σ band in MgB_2 single crystals is in the clean limit. At the same time, the π band, probed by c-axis tunneling, is moderately dirty, which is consistent with theoretical estimates [21]. Because of the increase of the effective coherence length at low energies [26,27], the dirty limit condition in the π band is certainly satisfied in the energy range $E < \Delta_{\max 2}$. This is consistent with the absence of localized states in the vortex core as claimed in Ref. [24].

The diffusion constants in MgB_2 are not known at present and may depend on the type of scatterers. In MgB_2 single crystals, available estimates of scattering rates [22] suggest that the σ band is in the clean limit and $\mathcal{D}_1 \gtrsim \mathcal{D}_2$. However, our results should still be qualitatively applicable even in this case. Indeed, if we focus on the DOS in the π band, which is in the dirty limit, then the Usadel equation for Green's function for this band is still valid. The only extra input required is the coordinate dependence of the pair potential Δ_1 in the σ band. The shape of this dependence of Δ_1 does not depend much on the degree of dirtiness; only the scale ξ_1 of this dependence changes. Since in the clean σ band ξ_1 is independent of $\mathcal{D}_1$, the $\mathcal{D}_1/\mathcal{D}_2$ ratio is not a relevant parameter. With ξ_1 defined as the typical scale of change of Δ_1, the plot in Fig. 4 is more general that the model used to obtain it. This resolves an apparent contradiction between our choice of $\mathcal{D}_{1,2}$ and transport data for MgB_2.

In conclusion, we studied the vortex core structure in a dirty two-band superconductor with weak interband scattering. The distributions of the order parameters and local DOS reveal two different spatial scales for the two bands, in qualitative agreement with recent STM experiments on MgB_2. This further supports the two-band model in MgB_2 and also provides an interesting new type of vortex core structure.

We acknowledge valuable discussions with A. Brinkman, O.V. Dolgov, I.I. Mazin, M. Iavarone, and G. Karapetrov. In Argonne this work was supported by the U.S. DOE, Office of Science, under Contract No. W-31-109-ENG-38.

[1] J. Nagamatsu *et al.*, Nature (London) **410**, 63 (2001).
[2] H. Suhl, B.T. Matthias, and L.R. Walker, Phys. Rev. Lett. **3**, 552 (1959).
[3] V.A. Moskalenko, Fiz. Met. Metalloved. **4**, 503 (1959).
[4] C.C. Sung and V.K. Wong, J. Phys. Chem. Solids **28**, 1933 (1967).
[5] N. Schopohl and K. Scharnberg, Solid State Commun. **22**, 371 (1977).
[6] A.A. Golubov and I.I. Mazin, Phys. Rev. B **55**, 15146 (1997).
[7] V.Z. Kresin and S.A. Wolf, Phys. Rev. B **41**, 4278 (1990); **46**, 6458 (1992); **51**, 1229 (1995).
[8] A.Y. Liu, I.I. Mazin, and J. Kortus, Phys. Rev. Lett. **87**, 87005 (2001).
[9] S.V. Shulga *et al.*, cond-mat/0103154.
[10] H.J. Choi *et al.*, Phys. Rev. B **66**, 020513 (2002); Nature (London) **418**, 758 (2002).
[11] A.A. Golubov *et al.*, J. Phys. Condens. Matter **14**, 1353 (2002).
[12] A. Brinkman *et al.*, Phys. Rev. B **65**, 180517 (2002).
[13] G. Binnig *et al.*, Phys. Rev. Lett. **45**, 1352 (1980).
[14] F. Giubileo *et al.*, Phys. Rev. Lett. **87**, 177008 (2001).
[15] M. Iavarone *et al.*, Phys. Rev. Lett. **89**, 187002 (2002).
[16] G. Rubio-Bollinger, H. Suderow, and S. Vieira, Phys. Rev. Lett. **86**, 5582 (2001); P. Martinez-Samper *et al.*, Physica (Amsterdam) **385C**, 233 (2003).
[17] P. Szabó *et al.*, Phys. Rev. Lett. **87**, 137005 (2001).
[18] H. Schmidt *et al.*, Phys. Rev. Lett. **88**, 127002 (2002).
[19] R.S. Gonnelli *et al.*, Phys. Rev. Lett. **89**, 247004 (2002).
[20] F. Bouquet *et al.*, Phys. Rev. Lett. **87**, 047001 (2001).
[21] I.I. Mazin *et al.*, Phys. Rev. Lett. **89**, 107002 (2002).
[22] E.A. Yelland *et al.*, Phys. Rev. Lett. **88**, 217002 (2002); J.R. Cooper *et al.*, Physica (Amsterdam) **385C**, 75 (2003).
[23] P. Miranović, K. Machida, and V.G. Kogan, cond-mat/0207146.
[24] M.R. Eskildsen *et al.*, Phys. Rev. Lett. **89**, 187003 (2002).
[25] N. Nakai, M. Ichioka, and K. Machida, J. Phys. Soc. Jpn. **71**, 23 (2002).
[26] K. Usadel, Phys. Rev. Lett. **25**, 507 (1970).
[27] L. Kramer, W. Pesch, and R.J. Watts-Tobin, J. Low Temp. Phys. **14**, 112 (1974).
[28] A.A. Golubov and M.Yu. Kupriyanov, J. Low Temp. Phys. **70**, 83 (1988).
[29] In many theoretical papers the model of "factorizable" interactions is used $\Lambda_{\alpha\beta} = g_\alpha g_\beta$ (see, e.g., Ref. [23]). This corresponds to the limit $W_{\alpha\beta} \to \infty$ with the fixed ratio $W_{21}/W_2 = W_1/W_{12}$. In this limit the gap ratio Δ_2/Δ_1 is rigidly fixed, leading to the model with a single order parameter distributed over the Fermi surface. We should note that there is no rigorous justification for this model, even though in many cases it catches essential physics.
[30] Ch. Renner *et al.*, Phys. Rev. Lett. **67**, 1650 (1991).